Phenolic Compounds Composition of *Hypericum perforatum* L. Wild-Growing Plants from the Republic of Macedonia

Oliver TUSEVSKI[1] (✉)
Marija KRSTIKJ[1]
Jasmina PETRESKA STANOEVA[2]
Marina STEFOVA[2]
Sonja GADZOVSKA SIMIC[1]

Summary

The aim of this study was to provide comprehensive understanding of phenolic compounds composition in roots (RO), non-flower shoots (NFS) and flower shoots (FS) of *Hypericum perforatum* wild-growing plants from the Republic of Macedonia. Identification of phenolic compounds in plant methanolic extracts was performed by HPLC-DAD/ESI-MS analysis. Chlorogenic acid and 3-p-coumaroylquinic acid were identified in NFS and FS, while 3-feruloylquinic acid was detected in RO and FS extracts. From the group of flavan-3-ols, (epi)catechin and procyanidins were found in all tested samples, whereas catechin and B-type procyanidin dimer were confirmed in NFS and FS. Four flavonol glycosides (hyperoside, rutin, quercitrin and kaempferol 3-*O*-rutinoside) were identified in aerial parts. Guaijaverin and kaempferol 3-*O*-glucoside were exclusively found in NFS. Quercetin, amentoflavone and I3-II8 biapigenin as flavonoid aglycones were detected only in FS extracts. The NFS and FS extracts showed a capability for the accumulation of cyanidin 3-*O*-glycoside and cyanidin 3-*O*-rhamnoside, as well for hyperforin and adhyperforin. Naphthodianthrones were represented with pseudohypericin, hypericin and protopseudohypericin in FS, while only hypericin was detected in NFS. Six xanthones, γ-mangostin, 5-*O*-methyl-2-deprenylrheediaxanthone B, garcinone C, 3,6-dihydroxy-1,5,7-trimethoxy-xanthone, cadensin G and cadensin C were exclusively confirmed in RO extracts. Padiaxanthone was detected in NFS, while dimethylmangiferin in FS extracts. The major finding of this study is the identification of novel xanthones in *H. perforatum* roots that could be potentially used as bioactive compounds in food and pharmaceutical industry.

Key words

HPLC/DAD/ESI-MS^n, *Hypericum perforatum* L., phenolic compounds

[1] Ss. Cyril and Methodius University in Skopje, Faculty of Natural Sciences and Mathematics, Department of Plant Physiology, Archimedova str. 3, 1000 Skopje, Republic of Macedonia
[2] Ss. Cyril and Methodius University in Skopje, Faculty of Natural Sciences and Mathematics, Department of Analytical Chemistry, Archimedova str. 3, 1000 Skopje, Republic of Macedonia

✉ Corresponding author: oliver.tusevski@pmf.ukim.mk

Received: May 19, 2018 | Accepted: October 19, 2018

Introduction

Hypericum perforatum L. (St. John's wort) represents one of the best-studied medicinal plants throughout the world with well-characterised bioactive metabolites and pharmacological activities. The *H. perforatum* extracts contain naphthodianthrones, acyl-phloroglucinols, flavonoids and xanthones with various pharmacological attributes that are associated with antidepressant, anti-inflammatory, hepatoprotective, antiviral, antimicrobial, antioxidant, antitumoral and wound-healing activities (Nahrstedt and Butterweck, 2010). Secondary metabolites (phenolic acids, flavonoids, hypericins and hyperforins) from *H. perforatum* that contribute to the biological activities are usually accumulated in leaves and flowers. There were strong indications that hyperforins are synthesized and accumulated in the translucent glands and their delimiting cells of the leaves, flowers and fruits (Soelberg et al., 2007). The hypericins are mainly localized in the dark glands dispersed over all aerial parts of *H. perforatum* plants, particularly on the margins of leaves and flower petals (Zobayed et al., 2006). Consequently, *H. perforatum* based products are prepared from Hyperici herba crude material as a natural source of bioactive compounds. Even the medicinal properties of Hyperici herba have been extensively studied (Nahrstedt and Butterweck, 2010; Velingkar et al., 2017), the chemical composition and biological activities of root extracts are rather scarce. Recently, phytochemical investigations on *H. perforatum* wild-growing plants demonstrated that roots are the main sites for accumulation of xanthones (Tocci et al., 2018). Nevertheless, the distribution of certain phenolic compounds in different aerial (stems, leaves, flowers, fruits) and underground parts (roots) of *H. perforatum* are not fully explored.

The objective of the present study was to search for different classes of phenolic compounds in *H. perforatum* roots (RO), non-flower shoots (NFS) and flower shoots (FS). This study revealed, for the first time, the co-presence of phenolic acids, flavan-3-ols and xanthones in RO extracts. Phenolic compounds in methanolic extracts were analyzed using high-performance liquid chromatography (HPLC) coupled with diode-array detection (DAD) and tandem mass spectrometry (MS^n) with electrospray ionization (ESI). The HPLC profiles obtained in the course of this work clearly evidenced a distinct phenolic profile between different parts of *H. perforatum* wild-growing plants.

Material and methods

Plant material

Plant material of *H. perforatum* was collected during full flowering time (July 2013) from a natural population in the National Park Pelister at about 1394 m a.s.l. Voucher specimen of the plant is deposited in the Herbarium at the Faculty of Natural Sciences and Mathematics, Ss. Cyril and Methodius University in Skopje, Republic of Macedonia (MKNH). The collected plant material was separated into three sections: roots (RO), non-flower shoots (NFS) and flower shoots (FS). Plant samples were air dried in darkness, ground to powder by laboratory mill, and stored in airtight containers for further analysis.

HPLC/DAD/ESI-MSn analysis of phenolic compounds

The plant extracts for identification and quantification of phenolic compounds were prepared when powdered material (0.2 g) was homogenized with 10 mL of 80% (v/v) CH_3OH in an ultrasonic bath for 30 min at 4°C (Gadzovska et al., 2013). Thereafter, methanolic extracts were centrifuged at 12,000 rpm for 15 min and the supernatants were used for HPLC/DAD/ESI–MS^n analysis.

The HPLC system was equipped with an Agilent 1100 series diode array and mass detector in series (Agilent Technologies, Waldbronn, Germany). Chromatographic separations were carried out on 150 x 4.6 mm, 5 µm XDB-C18 Eclipse column (Agilent, USA). The mobile phase consisted of two solvents: water-formic acid (A; 99:1, v/v) and methanol (B) in the following gradient program: 10% B (0–20 min), 20% B (20–30 min), 35 B (30–50 min), 50% B (50–70 min), 80% B (70–80 min) and continued with 100% B for a further 10 min. Each run was followed by an equilibration period of 10 min. The flow rate was 0.4 mL·min^{-1} and the injection volume 20 µL. All separations were performed at 38°C. The HPLC protocol was optimized for very complex matrices in order to obtain better separation of peaks (Tusevski et al., 2016; 2017). In this context, well-defined picks could be obtained by using higher temperature, but it should not be higher than 40°C, because it can cause degradation of polyphenolic compounds.

The commercial standards chlorogenic acid, rutin, quercetin, kaempferol, catechin, (epi)catechin, hypericin, pseudohypericin, hyperforin and xanthone were used as reference compounds. Spectral data from all peaks were accumulated in range 190-600 nm, and chromatograms were recorded at 260 nm for xanthones and hyperforins, at 280 nm for flavan-3-ols, at 330 nm for phenolic acids, at 350 nm for flavonols, at 520 nm for anthocyanins and at 590 nm for hypericins. In case of overlapping peaks in the DAD-chromatograms, separate quantification was possible with the help of the extracted ion chromatograms (EICs) at the *m/z* values of the corresponding molecular ions of each overlapping compound: the EIC integral value was used to estimate the contribution of each individual overlapping compound to the joint DAD peaks (Stanoeva et al., 2017).

The HPLC system was connected to the Agilent G2445A ion-trap mass spectrometer equipped with electrospray ionization (ESI) system and controlled by LCMSD software (Agilent, v.6.1.). Identification of the component peaks was based on the UV/Vis spectral data and LC/MS in the negative $[M–H]^-$ or positive $[M+H]^+$ (for anthocyanins) ionization mode with subsequent MS^2, MS^3 and MS^4 analysis for further identification with reference to similar data previously reported.

Results and discussion

The HPLC/DAD/ESI–MS^n technique was used to analyse the phenolic profile of RO, NFS and FS extracts of *H. perforatum* wild-growing plants (Fig. 1). Eight groups of phenolic compounds, such as phenolic acids, flavan-3-ols, flavonol glycosides, flavonoid aglycones, anthocyanins, naphthodianthrones, acyl-phloroglucinols and xanthones were recorded in the plant extracts.

Phenolic acids. The HPLC chromatograms confirmed the presence of four phenolic acids (F1, F2, F4 and F6) in the plant extracts that were identified by ESI–MS (Table 1). Compound **F1** with a molecular ion $[M–H]^-$ at *m/z* 191 was identified as quinic acid, taking into account its MS^n fragmentation pattern (Zhang

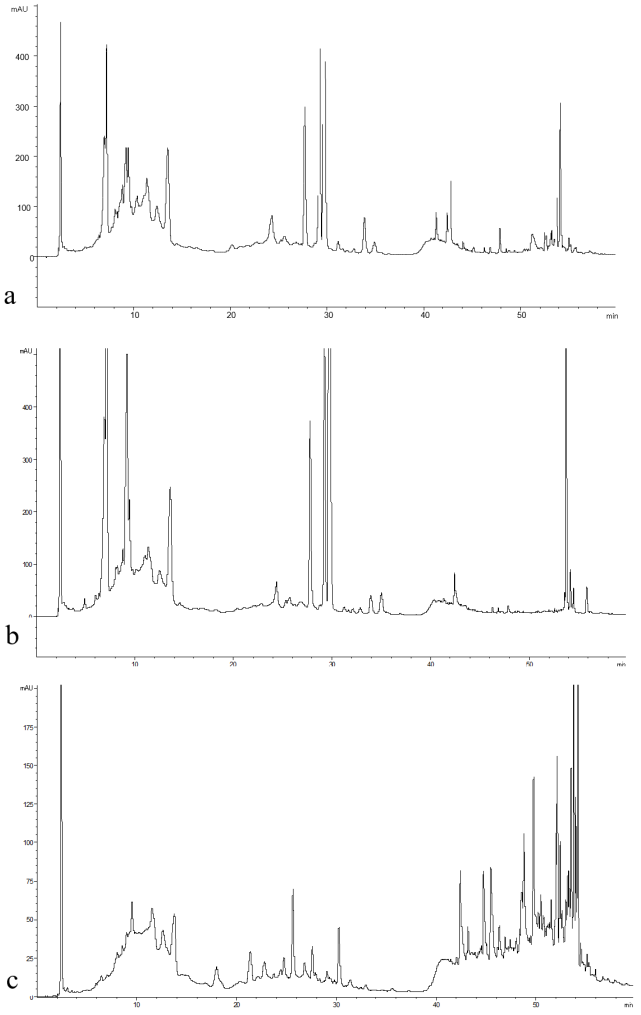

Figure 1. Chromatograms of *Hypericum perforatum* flower shoots (a), non-flower shoots (b) and roots (c) monitored at 280 nm for detection of phenolic compounds.

et al., 2007). The compounds **F2**, **F4** and **F6** were detected with identical UV spectra at 240–246 nm and 320-325 nm, and by a sharp diagnostic shoulder at 290–300 nm typical for compounds containing a caffeoyl group (Papetti et al., 2008). The full mass spectrum of chlorogenic acid/3-caffeoylquinic acid (**F2**) exhibited an intense $[M–H]^-$ ion at *m/z* 353 with fragment ions corresponding to quinic acid (base peak *m/z* 191) and caffeic acid (*m/z* 179) moieties. The 3-p-coumaroylquinic acid (**F4**) and 3-feruloylquinic acid (**F6**) were distinguished by their cinnamic acid derived MS^2 base peaks at *m/z* 163 and *m/z* 193, respectively. With respect to qualitative analysis, quinic acid was detected in all tested extracts. Chlorogenic acid and 3-p-coumaroylquinic acid were identified in FS and NFS, while their presence was not confirmed in RO extracts. Interestingly, 3-feruloylquinic acid was detected in RO and FS, but not in NFS extracts. Even the aerial parts of *H. perforatum* have been shown to accumulate various phenolic acids (Tusevski et al., 2016), this is the first report for the presence of quinic acid and 3-feruloylquinic acid in *H. perforatum* RO extracts.

Flavan-3-ols. The chromatographic analysis allowed the identification of 6 flavan-3-ols (F3, F5, F7-F9 and F12) in the plant extracts (Table 1). The mass spectrum of **F3** and **F9** in full scan mode showed $[M–H]^-$ at *m/z* 289, which corresponds to catechin and (epi)catechin, respectively (Tusevski et al., 2013). Numerous B-type procyanidin dimers (**F5**, **F8** and **F12**) with $[M–H]^-$ at *m/z* 577 were detected in the samples. The different retention time (t_R) of procyanidin dimers can be explained by the variations in inter-flavonoid bond linkages (B1, B2, B3), branch types (linear *versus* branched) and the combination/order of catechin and (epi) catechin monomers, which make up the dimer structure. The product ion spectrum of the deprotonated ion at *m/z* 577 produced several fragment ions: base peak at *m/z* 425 $[M–152–H]^-$ formed due to the retro Diels-Alder fragmentation and loss of the B ring, product ion at *m/z* 407 ($[M–152–18–H]^-$) due to the loss of water, probably by elimination of the 3OH, as well fragment ion at *m/z* 451 formed by elimination of the upper unit of dimer by heterocyclic ring fission fragmentation pathway. In addition, the formation of product ion at *m/z* 451 also indicates the presence of two hydroxyl group located at the C30 and C40 positions of the B ring. The upper and base units of this dimer were identified as (epi)catechin. Other minor product ions were observed at *m/z* 559 ($[M–18–H]^-$) due to loss of water from the dimer and *m/z* 289 ($[M–288–H]^-$) as a result from the cleavage of interflavan linkage through the quinone methide mechanism. The proanthocyanidins that consist exclusively of (epi)catechin are called procyanidins and the observed $[M–H]^-$ at *m/z* 577 is indicative of the B-type procyanidin dimer (Rodrigues et al., 2007). The compound **F7** with $[M–H]^-$ at *m/z* 865 and MS^2 fragment ions at *m/z* 739, 695 and 577 was assigned to procyanidin trimer. The observed base ion at *m/z* 695 due to a loss of 170 mass units correspond to the retro Diels-Alder fission with an additional loss of water, while the fragment ion at *m/z* 577 indicates a loss of 288 mass units characteristic for the interflavanic bond cleavage (Rockenbach et al., 2012). Among the detected flavan-3-ols, B-type procyanidin dimer (F5), procyanidin trimer and (epi)catechin were identified in all tested samples. Whilst catechin and B-type procyanidin dimer (F12) were only found in NFS and FS, another B-type procyanidin dimer (F8) was detected only in RO and FS. Even catechin and epicatechin have previously been detected in the aerial parts of *H. perforatum* (Ploss et al., 2001; Tusevski et al., 2016), the literature data for flavan-3-ol composition of *H. perforatum* roots are still limited. This study revealed, for the first time, the co-presence of epicatechin and procyanidin derivatives in *H. perforatum* RO extracts.

Flavonol glycosides. The presence of six flavonol glycosides (F13-F18) in the plant samples (Table 1) were represented with quercetin and kaempferol derivatives according to the characteristic UV spectra (257, 265sh and 355 nm) of flavonols glycosylated at C3. The compound **F13** had a $[M–H]^-$ at *m/z* 463 and its MS^2 gave a single ion at *m/z* 301 indicating that it is quercetin hexose derivative, probably hyperoside (quercetin 3-*O*-galactoside) (Silva et al., 2005). Taking into account the MS spectra, compounds F14 and F18 were distinguished as quercetin and kaempferol derivatives with rutinose at C3, respectively (Conceição et al., 2006). The absence of intermediate fragmentation between deprotonated molecular ion and aglycone ion is indicative of an interglycosidic linkage 1→6 (Cuyckens et al., 2001). Therefore, **F14** and **F18** were putatively identified as

Table 1. Identification of phenolic acids, flavan-3-ols, flavonol glycosides and flavonoid aglycones in *Hypericum perforatum* extracts

Peak	Phenolic compounds	t_R (min)	UV (nm)	$[M–H]^-$ (*m/z*)	MS^2 $[M–H]^-$ (*m/z*)	References	RO	NFS	FS
Phenolic acids									
F1	Quinic acid	6.50	262, 310	191	173, **127**	Zhang et al. (2007)	+	+	+
F2	Chlorogenic acid (3-caffeoylquinic acid)[a]	18.83	240, 294, 326	353	**191**, 179, 135	Pappeti et al. (2008)	-	+	+
F4	3-p-Coumaroylquinic acid	25.09	314	337	191, **163**	Pappeti et al. (2008)	-	+	+
F6	3-Feruloylquinic acid	29.11	314	367	193	Pappeti et al. (2008)	+	-	+
Flavan-3-ols									
F3	Catechin[a]	24.40	280	289	**245**, 205	Tusevski et al. (2013)	-	+	+
F5	B-type procyanidin dimer	27.89	280	577	559, 451, **425**, 407, 289	Rodrigues et al. (2007)	+	+	+
F7	Procyanidin trimer	31.08	280	865	739, **695**, 577	Rockenbach et al. (2012)	+	+	+
F8	B-type procyanidin dimer	31.26	280	577	559, 451, **425**, 407, 289	Rodrigues et al. (2007)	+	-	+
F9	(epi)catechin[a]	32.02	280	289	**245**, 205	Tusevski et al. (2013)	+	+	+
F12	B-type procyanidin dimer	37.29	280	577	559, 451, **425**, 407, 289	Rodrigues et al. (2007)	-	+	+
Flavonol glycosides and flavonoid aglycones									
F13	Hyperoside (quercetin 3-*O*-galactoside)	41.58	256, 356	469	**301**	Silva et al. (2005)	-	+	+
F14	Rutin (quercetin 3-*O*-rutinoside)	44.20	263, 298sh, 356	609	**301**	Conceição et al. 2006	-	+	+
F15	Guaijaverin (quercetin 3-*O*-arabinoside)	44.44	256, 294sh, 356	433	**301**	Rainha et al. 2013	-	+	-
F16	Kaempferol 3-*O*-glucoside	45.80	256, 266, 350	447	**285**	Tusevski et al. (2016)	-	+	-
F17	Quercitrin (quercetin 3-*O*-rhamnoside)	47.86	254, 354	447	**301**	Silva et al. (2005)	-	+	+
F18	Kaempferol 3-*O*-rutinoside	51.50	254, 268, 352	593	**285**	Conceição et al. 2006	-	+	+
F19	Quercetin[a]	54.70	256, 372	301	**179**, 151	Tusevski et al. (2013)	-	-	+
F20	I3–II8 Biapigenin	58.60	268, 336	537	443, 385, 151	Orčić et al. (2011)	-	-	+
F21	Amentoflavone	70.20	268, 336	537	443, 385, 151	Orčić et al. (2011)	-	-	+

t_R: retention time; RO: roots; NFS: non-flower shoots; FS: flower shoots; sh: shoulder; MS^2 ions in bold indicate the base peak
[a] Compounds identified with authentic standards

quercetin 3-*O*-rutinoside (rutin) and kaempferol 3-*O*-rutinoside, respectively. The compound **F15** was identified as quercetin pentoside, probably guaijaverin (quercetin 3-*O*-arabinoside) according to its $[M–H]^-$ at *m/z* 433 and MS^2 fragment ion at *m/z* 301 that corresponds to aglycone quercetin (Rainha et al., 2013). The compound F16 was identified as kaempferol derivative with glycosilation in position 3 according to its UV-spectra (256, 266 and 350 nm). The MS and MS^2 spectra were consistent with the presence of a hexose residue and confirmed the kaempferol aglycone. Therefore, compound **F16** was identified as kaempferol 3-*O*-glucoside (Tusevski et al., 2016). The compound **F17** showed UV-spectrum and MS data (Silva et al., 2005) consistent with those of quercitrin (quercetin 3-*O*-rhamnoside). All identified flavonol glycosides were confirmed in NFS and FS, but they were not detected in RO extracts. In accordance, flavonol glycosides (rutin, hyperoside, quercitrin and isoquercitrin) have been considered as specific biomarkers in the aerial parts of *H. perforatum* (Nahrstedt and Butterweck, 2010). Curiously, present results showed that guaijaverin and kaempferol 3-*O*-glucoside were exclusively found in NFS. In this view, guaijaverin has been accumulated in leaves rather than in reproductive tissues of *H. ternum* (Pinhatti et al., 2010).

Flavonoid aglycones. Three flavonoid aglycones (F19-F21) were detected only in FS extracts (Table 1). The identification of compound **F19** was confirmed by spiking with a commercial standard of quercetin and confirmation of its MS data (Tusevski et al., 2013). The compounds **F20** and **F21** showed molecular ion at *m/z* 537 that corresponds to I3–II8 biapigenin and amentoflavone, respectively. The identification was made by comparing their UV and MS spectra to those from literature data (Orčić et al., 2011). In accordance with the present results, quercetin and dimeric flavones have been found as common aglycones in the typical flavonoid spectrum of *H. perforatum* (Jürgenliemk and Nahrstedt, 2002; Bagdonaitė et al., 2012). Namely, the accumulation of quercetin and I3–II8 biapigenin in flower buds and blossoms of *H. perforatum* has been correlated with growth and development of reproductive organs (Filippini et al., 2010; Bagdonaitė et al., 2012).

Anthocyanins. The ESI/MS detection in positive mode was applied for identification of anthocyanins in plant extracts. According to t_R values, UV-Vis, MS spectra and literature data (Jürgenliemk and Nahrstedt, 2002; Mulinacci et al., 2008), the compounds F10 and F11 were identified as cyanidin derivatives (Table 2). The compound **F10** was identified as cyanidin 3-*O*-glucoside, since it showed a $[M+H]^+$ at *m/z* 449 and fragment ion *m/z* 287, which correspond to aglycone cyanidin. The $[M+H]^+$ of compound F11 was found at *m/z* 433 and fragment ion at *m/z* 287 indicated that the aglycon cyanidin was glycosylated with a deoxyhexose due to the loss of 146 mass units. Therefore, compound **F11** was identified as cyanidin 3-*O*-rhamnoside. Despite the potential for accumulation of cyanidin 3-*O*-glucoside and cyanidin 3-*O*-rhamnoside in FS and NFS samples, there is still lack of data for identification of anthocyanins in *H. perforatum*. To the best of our knowledge, cyanidin aglycone has been confirmed in *H. perforatum* extracts after acidic hydrolysis of cyanidin glycosides (Aybastier et al., 2013).

Naphthodianthrones. Among the class of naphthodianthrones, hypericin, pseudohypericin, and protopseudohypericin were identified in plant extracts (Table 2). The HPLC–MS analysis of

Table 2. Identification of anthocyanins, naphthodianthrones and acyl-phloroglucinols in *Hypericum perforatum* extracts.

Peak	Phenolic compounds	t_R (min)	UV (nm)	$[M–H]^-$ (*m/z*)	MS^2 $[M–H]^-$ (*m/z*)	References	RO	NFS	FS
F10	Cyanidin 3-*O*-glycoside	33.56	298, 520	449 $[M+H]^+$	**287**	Mulinacci et al. (2008); Jürgenliemk and Nahrstedt (2002)	-	+	+
F11	Cyanidin 3-*O*-rhamnoside	37.16	234, 280, 522	433 $[M+H]^+$	**287**	Mulinacci et al. (2008); Jürgenliemk and Nahrstedt (2002)	-	+	+
F22	Pseudohypericin[a]	81.70	234, 286, 326, 544, 590	519	487, 421	Tolonen et al. (2002); Piovan et al. (2004)	-	-	+
F23	Hypericin[a]	84.20	288, 325, 465, 590	503	**405**	Tolonen et al. (2002); Piovan et al. (2004)	-	+	+
F24	Protopseudohypericin	85.90	218, 254, 368, 542	521	477, **423**, 385, 317	Tolonen et al. (2002); Piovan et al. (2004)	-	-	+
F25	Hyperforin[a]	86.06	204, 224, 278	535	467, **383**, 315, 271	Tolonen et al. (2002); Piovan et al. (2004)	-	+	+
F26	Adhyperforin	86.49	206, 280	549	**397**	Tolonen et al. (2002); Piovan et al. (2004)		+	+

t_R: retention time; RO: roots; NFS: non-flower shoots; FS: flower shoots; sh: shoulder; MS^2 ions in bold indicate the base peak
[a] Compounds identified with authentic standards

F22-F24 gave fragment ion spectra identical to those previously reported (Piperopoulos et al., 1997; Tolonen et al., 2002; Piovan et al., 2004). Compound **F22** had a molecular ion at *m/z* 519. Its MS^2 fragmentation produced $[M\text{-}H\text{-}CH3OH]^-$ ion at *m/z* 487 and $[M\text{-}H\text{-}CH2{=}C{=}O\text{-}2CO]^-$ ion at *m/z* 421, indicating that this compound is pseudohypericin. Compound F23 had a molecular ion at *m/z* 503 and its MS^2 fragmentation gave an $[M\text{-}H\text{-}CH2{=}C{=}O\text{-}2CO]^-$ ion at *m/z* 405. The UV/DAD spectrum of compound **F23** showed four absorption maxima (288, 325, 465 and 590 nm), typical values for hypericin. The identity of this compound was verified by comparison of the ESI mass spectrum, UV/DAD spectrum, and the HPLC t_R with an authentic standard of hypericin. The ESI mass spectrum of compound F24 showed a molecular ion at *m/z* 521 and its MS^2 gave a single $[M\text{-}H\text{-}CH2{=}C{=}O\text{-}2CO]^-$ ion at *m/z* 423. The UV and mass spectra of compound **F24** were consisted with those of protopseudohypericin. The HPLC analysis showed that pseudohypericin, hypericin and protopseudohypericin were presented in FS extracts, while NFS produced only hypericin. In this context, the flower development in *H. perforatum* has been correlated to the relative abundance of dark glandular structures as the main accumulation sites of naphthodianthrones (Filippini et al., 2010).

Acyl-phloroglucinols. The chromatographic analyses of acyl-phloroglucinols resulted in the identification of hyperforin and adhyperforin in NFS and FS extracts (Table 2). The MS data of compound **F26** showed $[M–H]^-$ at *m/z* 549, while UV spectrum showed an absorption maximum at 280 nm. Its MS^2 fragmentation produced ion at *m/z* 397 corresponding to losses of $(CH_3)_2CCH(CH_2)_2$. All these data are consistent with the structure of adhyperforin (Tolonen et al., 2002; Piovan et al., 2004). For the compound **F25**, the ESI mass spectrum showed a molecular ion at *m/z* 535, which is for 14 amu less than in adhyperforin suggesting a difference in one methylene group (CH_2) with an identical UV spectrum; but eluted at an earlier time. These spectral data suggest the identity of this compound as hyperforin (Tolonen et al., 2002; Piovan et al., 2004). Present data for the identification of hyperforin and adhyperforin in NFS and FS extracts are in consonance with the observations of Gioti et al., (2009) indicating that hyperforins have been mainly accumulated in the aerial parts of *H. perforatum*.

Xanthones. Fourteen xanthones were detected in the plant extracts and nine of them were identified by ESI-MS (Table 3). These included simple oxygenated xanthones or derivatives with prenyl, pyran or methoxy groups. The compound **X2** was identified as padiaxanthone (brasilixanthone B) taking into account $[M–H]^-$ at *m/z* 391 and MS^2 fragment ions at *m/z* 377 and 359 (Ishiguro et al., 1996). The compound **X3** with $[M–H]^-$ at *m/z* 449 and daughter ions at *m/z* 315 and 301 were identified as dimethylmangiferin (Liu et al., 2011). The compound **X5** showed a molecular ion at *m/z* 317 and fragment ions at *m/z* 289 and 245, as well UV spectra (255, 310 and 340 nm) characteristic for 3,6-dihydroxy-1,5,7-trimethoxy xanthone (Chung et al., 2002). According to literature data (Bennett and Lee, 1989), compounds **X7** and **X14** with $[M–H]^-$ at *m/z* 481 were putatively identified as cadensin C and its isomer, respectively. The compound **X8** was identified as γ-mangostin (1,3,6,7-tetrahydroxyxanthone-C-bis-prenyl) with $[M–H]^-$ at *m/z* 395 (Tusevski et al., 2013). The identification of compound **X10** as 5-*O*-methyl-2-deprenylrheediaxanthone was conducted through comparison of MS data with those reported by Rath et al., (1996). The compound **X12** with $[M–H]^-$ at *m/z* 467 was tentatively identified as cadensin G (Tocci et al., 2011). The compound X13 showed $[M–H]^-$ at *m/z* 413 and its MS^2 spectra was generated by the loss of a prenyl residue C_4H_8 (56 amu) and two prenyl residues (112 amu). Therefore, compound **X13** was identified as garcinone C (Tusevski et al., 2016). Five detected compounds were not fully identified, but they were grouped into a class of xanthones based on their UV and MS spectra. Since the literature data for the compounds with similar fragmentation pattern are rather scarce, these compounds could be structurally classified as some xanthone derivatives. In addition, we have not commercially-available standards to make tentative identification and structural characterization of those compounds. Therefore, compounds **X1**, **X4**, **X6**, **X9** and **X11** were assigned as unknown xanthone derivatives (Table 3). The qualitative analysis showed the presence of 11 xanthones in RO extracts (X1, X4, X5, X7-X14), that were not confirmed in NFS and FS. It is worth to mention that garcinone C, γ-mangostin isomer, 3,6-dihydroxy-1,5,7-trimetoxy-xanthone, cadensin G and cadensin C were identified for the first time in *H. perforatum* roots. On the other hand, several xanthones with 1,3,5,6- and 1,3,6,7-oxigenation pattern have previously been identified in *H. perforatum* roots (Crockett et al., 2011; Tocci et al., 2013), but their presence was not confirmed in this study. Even mangiferin has previously been reported in the aerial parts of *H. perforatum* (Kitanov and Nedialkov, 1998), the potential interesting finding in this study was the identification of padiaxanthone in NFS and dimethylmangiferin in FS extracts. The chemotaxonomic importance of xanthones in *Hypericum* species has been intensively studied (Crockett and Robson, 2011); recent studies have been focused on the pharmacological properties of these compounds. Xanthones isolated from the genus *Hypericum* have been found to possess various biological activities including antioxidant, anti-inflammatory, antimicrobial and cytotoxic effects (Demirkiran, 2007; Tocci et al., 2018). Taking into account a high diversity of xanthones in *H. perforatum* RO samples, further investigations will be focused on the quantification of these compounds and their contribution to the biological activities of complex extracts.

Conclusion

In conclusion, we have established an efficient HPLC method for analysis of *H. perforatum* extracts allowing the simultaneous identification of various groups of phenolic compounds. Distinct phenolic profile between root, non-flower shoots and flower shoots of *H. perforatum* extracts was shown as detailed for the first time. The aerial plant samples synthesized hydroxycinnamic acid derivatives, flavan-3-ols, flavonols, naphthodianthrones and acyl-phloroglucinols. Root extracts showed biosynthetic potential for the production of specific phenolic compounds, such as quinic acid, 3-feruloylquinic acid, (epi)catechin, B-type procyanidin dimers and procyanidin trimer. More importantly, root extracts synthesized numerous xanthones that were not detected in non-flower shoot and flower shoot extracts. Therefore, *H. perforatum* roots could be considered as a promising source of xanthones that could be used as biologically active compounds in food and pharmaceutical industry.

Table 3. Identification of xanthones in *Hypericum perforatum* extracts.

Peak	Xanthones	t_R (min)	UV (nm)	$[M–H]^-$ (*m/z*)	MS^2 $[M–H]^-$ (*m/z*)	References	RO	NFS	FS
X1	Xanthone derivative 1	35.79	232, 286	557	539, 513, 417, 463, 297		+	-	-
X2	Padiaxanthone (brasilixanthone B)	37.93	254, 289, 330	391	377, 359	Ishiguro et al. (1996)	-	+	-
X3	Dimethylmangiferin	41.03	258, 319, 364	449	315, **301**, 285	Liu et al. (2011)	-	-	+
X4	Xanthone derivative 2	43.34	242, 306	367	**287**		+	-	-
X5	3,6-Dihydroxy-1,5,7-trimethoxy-xanthone	74.67	255, 310, 340	317	289, 245, 205, 180	Chung et al. (2002)	+	-	-
X6	Xanthone derivative 3	75.09	238, 256, 320	331	262, 234, 193		-	+	+
X7	Cadensin C	77.18	254, 284,326	481	**412**, 397, 234, 271, 327	Bennett and Lee (1989)	+	-	-
X8	γ-Mangostin isomer	80.43	254, 286, 324	395	325, 283, **271**	Tusevski et al. (2013)	+	-	-
X9	Xanthone derivative 4	82.56	206, 252, 326	345	276, 233		+	-	-
X10	5-*O*-Methyl-2-deprenylrheediaxanthone B	82.60	252, 286, 330	331	262, 234, 193	Rath et al. (1996)	+	-	-
X11	Xanthone derivative 5	83.65	206, 232, 278, 336	399	331, 287		+	-	-
X12	Cadensin G	84.16	270, 330, 400	467	257, 227	Tocci et al. (2011)	+	-	-
X13	Garcinone C	84.20	286, 340	413	344, **301**	Tusevski et al. (2016)	+	-	-
X14	Cadensin C isomer	84.65	254, 284, 326	481	412, 397, 234, 271, 327	Bennett and Lee (1989)	+	-	-

t_R: retention time; RO: roots; NFS: non-flower shoots; FS: flower shoots; sh: shoulder; MS^2 ions in bold indicate the base peak

References

Aybastıer Ö., Şahin S., Demir C. (2013). Response surface optimized ultrasonic-assisted extraction of quercetin and isolation of phenolic compounds from *Hypericum perforatum* L. by column chromatography. Sep Sci Technol 48 (11): 1665-1674.

Bagdonaitė E., Mártonfi P., Repčák M., Labokas J. (2012). Variation in concentrations of major bioactive compounds in *Hypericum perforatum* L. from Lithuania. Ind Crops Prod 35 (1): 302-308.

Bennett G. J., Lee H. H. (1989). Xanthones from guttiferae. Phytochemistry 28 (4): 967-998.

Chung M. I., Weng J. R., Wang J. P., Teng C. M., Lin C. N. (2002). Antiplatelet and anti-inflammatory constituents and new oxygenated xanthones from *Hypericum geminiflorum*. Planta Med 68 (01): 25-29.

Conceiçao L. F., Ferreres F., Tavares R. M., Dias A. C. (2006). Induction of phenolic compounds in *Hypericum perforatum* L. cells by *Colletotrichum gloeosporioides* elicitation. Phytochemistry 67 (2): 149-155.

Crockett S. L., Poller B., Tabanca N., Pferschy-Wenzig E. M., Kunert O., Wedge D. E., Bucar F. (2011). Bioactive xanthones from the roots of *Hypericum perforatum* (common St John's wort). J Sci Food Agric 91 (3): 428-434.

Crockett, S. L., Robson, N. K. (2011). Taxonomy and chemotaxonomy of the genus *Hypericum*. Medicinal and aromatic plant science and biotechnology, 5(1), 1.

Cuyckens F., Rozenberg R., de Hoffmann E., Claeys M. (2001). Structure characterization of flavonoid O-diglycosides by positive and negative nano-electrospray ionization ion trap mass spectrometry. J Mass Spectrom 36 (11): 1203-1210.

Demirkiran, O. (2007). Xanthones in *Hypericum*: synthesis and biological activities. In Bioactive Heterocycles III (pp. 139-178). Springer, Berlin, Heidelberg.

Filippini R., Piovan A., Borsarini A., Caniato R. (2010). Study of dynamic accumulation of secondary metabolites in three subspecies of *Hypericum perforatum*. Fitoterapia 81 (2): 115-119.

Gadzovska S., Maury S., Delaunay A., Spasenoski M., Hagège D., Courtois D., Joseph C. (2013). The influence of salicylic acid elicitation of shoots, callus, and cell suspension cultures on production of naphtodianthrones and phenylpropanoids in *Hypericum perforatum* L. Plant Cell Tiss Org Cult 113 (1): 25-39.

Gioti E. M., Fiamegos Y. C., Skalkos D. C., Stalikas C. D. (2009). Antioxidant activity and bioactive components of the aerial parts of *Hypericum perforatum* L. from Epirus, Greece. Food Chem 117 (3): 398-404.

Ishiguro K., Fukumoto H., Suitani A., Nakajima M., Isoi K. (1996). Prenylated xanthones from cell suspension cultures of *Hypericum patulum*. Phytochemistry 42 (2): 435-437.

Jürgenliemk G., Nahrstedt A. (2002). Phenolic compounds from *Hypericum perforatum*. Planta Med 68 (01): 88-91.

Kitanov G. M., Nedialkov P. T. (1998). Mangiferin and isomangiferin in some *Hypericum* species. Biochem Syst Ecol 26 (6): 647-653.

Liu H., Wang K., Tang Y., Sun Z., Jian L., Li Z., Wu B., Huang C. (2011). Structure elucidation of *in vivo* and *in vitro* metabolites of mangiferin. J Pharm Biomed Anal 55 (5): 1075-1082.

Mulinacci N., Giaccherini C., Santamaria A. R., Caniato R., Ferrari F., Valletta A., Vincieri F. F., Pasqua G. (2008). Anthocyanins and xanthones in the calli and regenerated shoots of *Hypericum perforatum* var. *angustifolium* (sin. Fröhlich) Borkh. Plant Physiol Biochem 46 (4): 414-420.

Nahrstedt A., Butterweck V. (2010). Lessons Learned from Herbal Medicinal Products: The Example of St. John's Wort. J Nat Prod 73 (5): 1015-1021.

Orčić D. Z., Mimica-Dukić N. M., Francišković M. M., Petrović S. S., Jovin E. Đ. (2011). Antioxidant activity relationship of phenolic compounds in *Hypericum perforatum* L. Chem Cent J 5 (1): 1-8.

Papetti A., Daglia M., Aceti C., Sordelli B., Spini V., Carazzone C., Gazzani G. (2008). Hydroxycinnamic acid derivatives occurring in *Cichorium endivia* vegetables. J Pharm Biomed Anal 48 (2): 472-476.

Stanoeva, J. P., Stefova, M., Andonovska, K. B., Vankova, A., & Stafilov, T. (2017). Phenolics and mineral content in bilberry and bog bilberry from Macedonia. Int J Food Prop 20(sup1): S863-S883.

Pinhatti A. V., de Matos Nunes J., Maurmann N., Rosa L. M. G., von Poser G. L., Rech S. B. (2010). Phenolic compounds accumulation in *Hypericum ternum* propagated *in vitro* and during plant development acclimatization. Acta Physiol Plant 32 (4): 675-681.

Piovan A., Filippini R., Caniato R., Borsarini A., Maleci L. B., Cappelletti E. M. (2004). Detection of hypericins in the "red glands" of *Hypericum elodes* by ESI–MS/MS. Phytochemistry 65 (4): 411-414.

Piperopoulos G., Lotz R., Wixforth A., Schmierer T., Zeller K. P. (1997). Determination of naphthodianthrones in plant extracts from *Hypericum perforatum* L. by liquid chromatography–electrospray mass spectrometry. Journal Chromatogr B: Biomed Sci Appl 695 (2): 309-316.

Ploss O., Petereit F., Nahrstedt A. (2001). Procyanidins from the herb of *Hypericum perforatum*. Pharmazie 56 (6): 509-511.

Rainha N., Koci K., Coelho A. V., Lima E., Baptista J., Fernandes-Ferreira M. (2013). HPLC–UV–ESI-MS analysis of phenolic compounds and antioxidant properties of *Hypericum undulatum* shoot cultures and wild-growing plants. Phytochemistry 86: 83-91.

Rath G., Potterat O., Mavi S., Hostettmann K. (1996). Xanthones from *Hypericum roeperanum*. Phytochemistry 43 (2): 513-520.

Rockenbach I. I., Jungfer E., Ritter C., Santiago-Schübel B., Thiele B., Fett R., Galensa R. (2012). Characterization of flavan-3-ols in seeds of grape pomace by CE, HPLC-DAD-MS^n and LC-ESI-FTICR-MS. Food Res Int 48 (2): 848-855.

Rodrigues C. M., Rinaldo D., dos Santos L. C., Montoro P., Piacente S., Pizza C., Hiruma-Lima C. A., Brito A. R., Vilegas W. (2007). Metabolic fingerprinting using direct flow injection electrospray ionization tandem mass spectrometry for the characterization of proanthocyanidins from the barks of *Hancornia speciosa*. Rapid Commun Mass Spectrom 21 (12): 1907-1914.

Silva B. A., Ferreres F., Malva J. O., Dias A. C. (2005). Phytochemical and antioxidant characterization of *Hypericum perforatum* alcoholic extracts. Food Chem 90 (1): 157-167.

Soelberg J., Jørgensen L. B., Jäger A. K. (2007). Hyperforin accumulates in the translucent glands of *Hypericum perforatum*. Ann Bot 99 (6): 1097-1100.

Tocci N., Gaid M., Kaftan F., Belkheir A. K., Belhadj I., Liu B., Svatoš A., Hänsch R., Pasqua G., Beerhues L. (2018). Exodermis and endodermis are the sites of xanthone biosynthesis in *Hypericum perforatum* roots. New Phytol 217 (3): 1099-1112.

Tocci N., Simonetti G., D'Auria F. D., Panella S., Palamara A. T., Valletta A., Pasqua G. (2011). Root cultures of *Hypericum perforatum* subsp. angustifolium elicited with chitosan and production of xanthone-rich extracts with antifungal activity. Appl Microbiol Biotechnol 91 (4): 977-987.

Tocci N., Simonetti G., D'Auria F. D., Panella S., Palamara A. T., Ferrari F., Pasqua G. (2013). Chemical composition and antifungal activity of *Hypericum perforatum* subsp. *angustifolium* roots from wild plants and plants grown under controlled conditions. Plant Biosystems 147 (3): 557-562.

Tolonen A., Uusitalo J., Hohtola A., Jalonen J. (2002). Determination of naphthodianthrones and phloroglucinols from *Hypericum perforatum* extracts by liquid chromatography/tandem mass spectrometry. Rapid Commun Mass Spectrom 16 (5): 396-402.

Tusevski O., Stanoeva J. P., Markoska E., Brndevska N., Stefova M., Gadzovska Simic S. (2016). Callus cultures of *Hypericum perforatum* L. a novel and efficient source for xanthone production. Plant Cell Tiss Org Cult 125 (2): 309-319.

Tusevski O., Stanoeva J., Stefova M., Kungulovski D., Pancevska N., Sekulovski N., Panov S., Gadzovska Simic S. (2013). Hairy roots of *Hypericum perforatum* L.: a promising system for xanthone production. Open Life Sci 8 (10): 1010-1022.

Tusevski, O., Vinterhalter, B., Milošević, D. K., Soković, M., Ćirić, A., Vinterhalter, D., Zdravković Korać, S., Petreska Stanoeva J., Stefova, M., Gadzovska Simic, S. (2017). Production of phenolic compounds, antioxidant and antimicrobial activities in hairy root and shoot cultures of *Hypericum perforatum* L. Plant Cell Tiss Org Cult 128(3), 589-605.

Velingkar V. S., Gupta G. L., Hegde N. B. (2017). A current update on phytochemistry, pharmacology and herb–drug interactions of *Hypericum perforatum*. Phytochem Rev 16 (4): 725-744.

Zhang Y., Shi P., Qu H., Cheng Y. (2007). Characterization of phenolic compounds in *Erigeron breviscapus* by liquid chromatography coupled to electrospray ionization mass spectrometry. Rapid Commun Mass Spectrom 21 (18): 2971-2984.

Zobayed S. M. A., Afreen F., Goto E., Kozai T. (2006). Plant–environment interactions: accumulation of hypericin in dark glands of *Hypericum perforatum*. Ann Bot 98 (4): 793-804.

aCS84_09